SemiLep-06/17

BAD 2060, version 9

Collaboration-Wide Review

10 July 2008 to 24 July 2008

Primary BAD	2060, version 9 `Measurement of the B -> omega l nu and B -> eta l nu branching fractions using neutrino reconstruction.`
Author list	Anders, Christoph F.; Dingfelder, Jochen Christian; Langenbruch, Christoph; Uwer, Ulrich; Walker, Paul Andreas
Review Committee	comm409, members: Bozzi, Concezio; Feltresi, Enrico; Taras, Paul (chair)
Target	Physical Review D - Rapid Communications
Result type	
Supporting BAD(s)	BAD #2007 `Measurement of the B -> omega l nu and B -> eta l nu branching fractions using neutrino reconstruction.`
Changes since preliminary result	
BAIS/CWR Comments	
Institutional Reading Groups	2b. Budker, UCLA, Colorado, Royal Holloway, McGill, MIT, Trieste 6b. Edinburgh, Liverpool, Milan, Stanford, UT Austin, Wisconsin

Cover page generated by BAIS on July 10, 2008

Measurement of the $B^+ \to \omega\ell^+\nu$ and $B^+ \to \eta\ell^+\nu$ Branching Fractions

B. Aubert,[1] M. Bona,[1] Y. Karyotakis,[1] J. P. Lees,[1] V. Poireau,[1] E. Prencipe,[1] X. Prudent,[1] V. Tisserand,[1] J. Garra Tico,[2] E. Grauges,[2] L. Lopez[ab],[3] A. Palano[ab],[3] M. Pappagallo[ab],[3] G. Eigen,[4] B. Stugu,[4] L. Sun,[4] G. S. Abrams,[5] M. Battaglia,[5] D. N. Brown,[5] R. N. Cahn,[5] R. G. Jacobsen,[5] L. T. Kerth,[5] Yu. G. Kolomensky,[5] G. Lynch,[5] I. L. Osipenkov,[5] M. T. Ronan,[5,*] K. Tackmann,[5] T. Tanabe,[5] C. M. Hawkes,[6] N. Soni,[6] A. T. Watson,[6] H. Koch,[7] T. Schroeder,[7] D. Walker,[8] D. J. Asgeirsson,[9] B. G. Fulsom,[9] C. Hearty,[9] T. S. Mattison,[9] J. A. McKenna,[9] M. Barrett,[10] A. Khan,[10] V. E. Blinov,[11] A. D. Bukin,[11] A. R. Buzykaev,[11] V. P. Druzhinin,[11] V. B. Golubev,[11] A. P. Onuchin,[11] S. I. Serednyakov,[11] Yu. I. Skovpen,[11] E. P. Solodov,[11] K. Yu. Todyshev,[11] M. Bondioli,[12] S. Curry,[12] I. Eschrich,[12] D. Kirkby,[12] A. J. Lankford,[12] P. Lund,[12] M. Mandelkern,[12] E. C. Martin,[12] D. P. Stoker,[12] S. Abachi,[13] C. Buchanan,[13] J. W. Gary,[14] F. Liu,[14] O. Long,[14] B. C. Shen,[14,*] G. M. Vitug,[14] Z. Yasin,[14] L. Zhang,[14] V. Sharma,[15] C. Campagnari,[16] T. M. Hong,[16] D. Kovalskyi,[16] M. A. Mazur,[16] J. D. Richman,[16] T. W. Beck,[17] A. M. Eisner,[17] C. J. Flacco,[17] C. A. Heusch,[17] J. Kroseberg,[17] W. S. Lockman,[17] A. J. Martinez,[17] T. Schalk,[17] B. A. Schumm,[17] A. Seiden,[17] M. G. Wilson,[17] L. O. Winstrom,[17] C. H. Cheng,[18] D. A. Doll,[18] B. Echenard,[18] F. Fang,[18] D. G. Hitlin,[18] I. Narsky,[18] T. Piatenko,[18] F. C. Porter,[18] R. Andreassen,[19] G. Mancinelli,[19] B. T. Meadows,[19] K. Mishra,[19] M. D. Sokoloff,[19] P. C. Bloom,[20] W. T. Ford,[20] A. Gaz,[20] J. F. Hirschauer,[20] M. Nagel,[20] U. Nauenberg,[20] J. G. Smith,[20] K. A. Ulmer,[20] S. R. Wagner,[20] R. Ayad,[21,†] A. Soffer,[21,‡] W. H. Toki,[21] R. J. Wilson,[21] D. D. Altenburg,[22] E. Feltresi,[22] A. Hauke,[22] H. Jasper,[22] M. Karbach,[22] J. Merkel,[22] A. Petzold,[22] B. Spaan,[22] K. Wacker,[22] M. J. Kobel,[23] W. F. Mader,[23] R. Nogowski,[23] K. R. Schubert,[23] R. Schwierz,[23] A. Volk,[23] D. Bernard,[24] G. R. Bonneaud,[24] E. Latour,[24] M. Verderi,[24] P. J. Clark,[25] S. Playfer,[25] J. E. Watson,[25] M. Andreotti[ab],[26] D. Bettoni[a],[26] C. Bozzi[a],[26] R. Calabrese[ab],[26] A. Cecchi[ab],[26] G. Cibinetto[ab],[26] P. Franchini[ab],[26] E. Luppi[ab],[26] M. Negrini[ab],[26] A. Petrella[ab],[26] L. Piemontese[a],[26] V. Santoro[ab],[26] R. Baldini-Ferroli,[27] A. Calcaterra,[27] R. de Sangro,[27] G. Finocchiaro,[27] S. Pacetti,[27] P. Patteri,[27] I. M. Peruzzi,[27,§] M. Piccolo,[27] M. Rama,[27] A. Zallo,[27] A. Buzzo[a],[28] R. Contri[ab],[28] M. Lo Vetere[ab],[28] M. M. Macri[a],[28] M. R. Monge[ab],[28] S. Passaggio[a],[28] C. Patrignani[ab],[28] E. Robutti[a],[28] A. Santroni[ab],[28] S. Tosi[ab],[28] K. S. Chaisanguanthum,[29] M. Morii,[29] A. Adametz,[30] C. Anders,[30] C. Langenbruch,[30] J. Marks,[30] S. Schenk,[30] U. Uwer,[30] V. Klose,[31] H. M. Lacker,[31] D. J. Bard,[32] P. D. Dauncey,[32] J. A. Nash,[32] M. Tibbetts,[32] P. K. Behera,[33] X. Chai,[33] M. J. Charles,[33] U. Mallik,[33] J. Cochran,[34] H. B. Crawley,[34] L. Dong,[34] W. T. Meyer,[34] S. Prell,[34] E. I. Rosenberg,[34] A. E. Rubin,[34] Y. Y. Gao,[35] A. V. Gritsan,[35] Z. J. Guo,[35] C. K. Lae,[35] N. Arnaud,[36] J. Béquilleux,[36] A. D'Orazio,[36] M. Davier,[36] J. Firmino da Costa,[36] G. Grosdidier,[36] A. Höcker,[36] V. Lepeltier,[36] F. Le Diberder,[36] A. M. Lutz,[36] S. Pruvot,[36] P. Roudeau,[36] M. H. Schune,[36] J. Serrano,[36] V. Sordini,[36,¶] A. Stocchi,[36] G. Wormser,[36] D. J. Lange,[37] D. M. Wright,[37] I. Bingham,[38] J. P. Burke,[38] C. A. Chavez,[38] J. R. Fry,[38] E. Gabathuler,[38] R. Gamet,[38] D. E. Hutchcroft,[38] D. J. Payne,[38] C. Touramanis,[38] A. J. Bevan,[39] C. K. Clarke,[39] K. A. George,[39] F. Di Lodovico,[39] R. Sacco,[39] M. Sigamani,[39] G. Cowan,[40] H. U. Flaecher,[40] D. A. Hopkins,[40] S. Paramesvaran,[40] F. Salvatore,[40] A. C. Wren,[40] D. N. Brown,[41] C. L. Davis,[41] A. G. Denig,[42] M. Fritsch,[42] W. Gradl,[42] G. Schott,[42] K. E. Alwyn,[43] D. Bailey,[43] R. J. Barlow,[43] Y. M. Chia,[43] C. L. Edgar,[43] G. Jackson,[43] G. D. Lafferty,[43] T. J. West,[43] J. I. Yi,[43] J. Anderson,[44] C. Chen,[44] A. Jawahery,[44] D. A. Roberts,[44] G. Simi,[44] J. M. Tuggle,[44] C. Dallapiccola,[45] X. Li,[45] E. Salvati,[45] S. Saremi,[45] R. Cowan,[46] D. Dujmic,[46] P. H. Fisher,[46] G. Sciolla,[46] M. Spitznagel,[46] F. Taylor,[46] R. K. Yamamoto,[46] M. Zhao,[46] P. M. Patel,[47] S. H. Robertson,[47] A. Lazzaro[ab],[48] V. Lombardo[a],[48] F. Palombo[ab],[48] J. M. Bauer,[49] L. Cremaldi,[49] R. Godang,[49,**] R. Kroeger,[49] D. A. Sanders,[49] D. J. Summers,[49] H. W. Zhao,[49] M. Simard,[50] P. Taras,[50] F. B. Viaud,[50] H. Nicholson,[51] G. De Nardo[ab],[52] L. Lista[a],[52] D. Monorchio[ab],[52] G. Onorato[ab],[52] C. Sciacca[ab],[52] G. Raven,[53] H. L. Snoek,[53] C. P. Jessop,[54] K. J. Knoepfel,[54] J. M. LoSecco,[54] W. F. Wang,[54] G. Benelli,[55] L. A. Corwin,[55] K. Honscheid,[55] H. Kagan,[55] R. Kass,[55] J. P. Morris,[55] A. M. Rahimi,[55] J. J. Regensburger,[55] S. J. Sekula,[55] Q. K. Wong,[55] N. L. Blount,[56] J. Brau,[56] R. Frey,[56] O. Igonkina,[56] J. A. Kolb,[56] M. Lu,[56] R. Rahmat,[56] N. B. Sinev,[56] D. Strom,[56] J. Strube,[56] E. Torrence,[56] G. Castelli[ab],[57] N. Gagliardi[ab],[57] M. Margoni[ab],[57] M. Morandin[a],[57] M. Posocco[a],[57] M. Rotondo[a],[57] F. Simonetto[ab],[57] R. Stroili[ab],[57] C. Voci[ab],[57] P. del Amo Sanchez,[58] E. Ben-Haim,[58] H. Briand,[58] G. Calderini,[58] J. Chauveau,[58] P. David,[58] L. Del Buono,[58]

O. Hamon,[58] Ph. Leruste,[58] J. Ocariz,[58] A. Perez,[58] J. Prendki,[58] S. Sitt,[58] L. Gladney,[59] M. Biasini[ab],[60] R. Covarelli[ab],[60] E. Manoni[ab],[60] C. Angelini[ab],[61] G. Batignani[ab],[61] S. Bettarini[ab],[61] M. Carpinelli[ab],[61, ††] A. Cervelli[ab],[61] F. Forti[ab],[61] M. A. Giorgi[ab],[61] A. Lusiani[ac],[61] G. Marchiori[ab],[61] M. Morganti[ab],[61] N. Neri[ab],[61] E. Paoloni[ab],[61] G. Rizzo[ab],[61] J. J. Walsh[a],[61] D. Lopes Pegna,[62] C. Lu,[62] J. Olsen,[62] A. J. S. Smith,[62] A. V. Telnov,[62] F. Anulli[a],[63] E. Baracchini[ab],[63] G. Cavoto[a],[63] D. del Re[ab],[63] E. Di Marco[ab],[63] R. Faccini[ab],[63] F. Ferrarotto[a],[63] F. Ferroni[ab],[63] M. Gaspero[ab],[63] P. D. Jackson[a],[63] L. Li Gioi[a],[63] M. A. Mazzoni[a],[63] S. Morganti[a],[63] G. Piredda[a],[63] F. Polci[ab],[63] F. Renga[ab],[63] C. Voena[a],[63] M. Ebert,[64] T. Hartmann,[64] H. Schröder,[64] R. Waldi,[64] T. Adye,[65] B. Franek,[65] E. O. Olaiya,[65] F. F. Wilson,[65] S. Emery,[66] M. Escalier,[66] L. Esteve,[66] S. F. Ganzhur,[66] G. Hamel de Monchenault,[66] W. Kozanecki,[66] G. Vasseur,[66] Ch. Yèche,[66] M. Zito,[66] X. R. Chen,[67] H. Liu,[67] W. Park,[67] M. V. Purohit,[67] R. M. White,[67] J. R. Wilson,[67] M. T. Allen,[68] D. Aston,[68] R. Bartoldus,[68] P. Bechtle,[68] J. F. Benitez,[68] R. Cenci,[68] J. P. Coleman,[68] M. R. Convery,[68] J. C. Dingfelder,[68] J. Dorfan,[68] G. P. Dubois-Felsmann,[68] W. Dunwoodie,[68] R. C. Field,[68] A. M. Gabareen,[68] S. J. Gowdy,[68] M. T. Graham,[68] P. Grenier,[68] C. Hast,[68] W. R. Innes,[68] J. Kaminski,[68] M. H. Kelsey,[68] H. Kim,[68] P. Kim,[68] M. L. Kocian,[68] D. W. G. S. Leith,[68] S. Li,[68] B. Lindquist,[68] S. Luitz,[68] V. Luth,[68] H. L. Lynch,[68] D. B. MacFarlane,[68] H. Marsiske,[68] R. Messner,[68] D. R. Muller,[68] H. Neal,[68] S. Nelson,[68] C. P. O'Grady,[68] I. Ofte,[68] A. Perazzo,[68] M. Perl,[68] B. N. Ratcliff,[68] A. Roodman,[68] A. A. Salnikov,[68] R. H. Schindler,[68] J. Schwiening,[68] A. Snyder,[68] D. Su,[68] M. K. Sullivan,[68] K. Suzuki,[68] S. K. Swain,[68] J. M. Thompson,[68] J. Va'vra,[68] A. P. Wagner,[68] M. Weaver,[68] C. A. West,[68] W. J. Wisniewski,[68] M. Wittgen,[68] D. H. Wright,[68] H. W. Wulsin,[68] A. K. Yarritu,[68] K. Yi,[68] C. C. Young,[68] V. Ziegler,[68] P. R. Burchat,[69] A. J. Edwards,[69] S. A. Majewski,[69] T. S. Miyashita,[69] B. A. Petersen,[69] L. Wilden,[69] S. Ahmed,[70] M. S. Alam,[70] J. A. Ernst,[70] B. Pan,[70] M. A. Saeed,[70] S. B. Zain,[70] S. M. Spanier,[71] B. J. Wogsland,[71] R. Eckmann,[72] J. L. Ritchie,[72] A. M. Ruland,[72] C. J. Schilling,[72] R. F. Schwitters,[72] B. W. Drummond,[73] J. M. Izen,[73] X. C. Lou,[73] F. Bianchi[ab],[74] D. Gamba[ab],[74] M. Pelliccioni[ab],[74] M. Bomben[ab],[75] L. Bosisio[ab],[75] C. Cartaro[ab],[75] G. Della Ricca[ab],[75] L. Lanceri[ab],[75] L. Vitale[ab],[75] V. Azzolini,[76] N. Lopez-March,[76] F. Martinez-Vidal,[76] D. A. Milanes,[76] A. Oyanguren,[76] J. Albert,[77] Sw. Banerjee,[77] B. Bhuyan,[77] H. H. F. Choi,[77] K. Hamano,[77] R. Kowalewski,[77] M. J. Lewczuk,[77] I. M. Nugent,[77] J. M. Roney,[77] R. J. Sobie,[77] T. J. Gershon,[78] P. F. Harrison,[78] J. Ilic,[78] T. E. Latham,[78] G. B. Mohanty,[78] H. R. Band,[79] X. Chen,[79] S. Dasu,[79] K. T. Flood,[79] Y. Pan,[79] M. Pierini,[79] R. Prepost,[79] C. O. Vuosalo,[79] and S. L. Wu[79]

(The BABAR Collaboration)

[1]Laboratoire de Physique des Particules, IN2P3/CNRS et Université de Savoie, F-74941 Annecy-Le-Vieux, France
[2]Universitat de Barcelona, Facultat de Fisica, Departament ECM, E-08028 Barcelona, Spain
[3]INFN Sezione di Bari[a]; Dipartmento di Fisica, Università di Bari[b], I-70126 Bari, Italy
[4]University of Bergen, Institute of Physics, N-5007 Bergen, Norway
[5]Lawrence Berkeley National Laboratory and University of California, Berkeley, California 94720, USA
[6]University of Birmingham, Birmingham, B15 2TT, United Kingdom
[7]Ruhr Universität Bochum, Institut für Experimentalphysik 1, D-44780 Bochum, Germany
[8]University of Bristol, Bristol BS8 1TL, United Kingdom
[9]University of British Columbia, Vancouver, British Columbia, Canada V6T 1Z1
[10]Brunel University, Uxbridge, Middlesex UB8 3PH, United Kingdom
[11]Budker Institute of Nuclear Physics, Novosibirsk 630090, Russia
[12]University of California at Irvine, Irvine, California 92697, USA
[13]University of California at Los Angeles, Los Angeles, California 90024, USA
[14]University of California at Riverside, Riverside, California 92521, USA
[15]University of California at San Diego, La Jolla, California 92093, USA
[16]University of California at Santa Barbara, Santa Barbara, California 93106, USA
[17]University of California at Santa Cruz, Institute for Particle Physics, Santa Cruz, California 95064, USA
[18]California Institute of Technology, Pasadena, California 91125, USA
[19]University of Cincinnati, Cincinnati, Ohio 45221, USA
[20]University of Colorado, Boulder, Colorado 80309, USA
[21]Colorado State University, Fort Collins, Colorado 80523, USA
[22]Technische Universität Dortmund, Fakultät Physik, D-44221 Dortmund, Germany
[23]Technische Universität Dresden, Institut für Kern- und Teilchenphysik, D-01062 Dresden, Germany
[24]Laboratoire Leprince-Ringuet, CNRS/IN2P3, Ecole Polytechnique, F-91128 Palaiseau, France
[25]University of Edinburgh, Edinburgh EH9 3JZ, United Kingdom
[26]INFN Sezione di Ferrara[a]; Dipartimento di Fisica, Università di Ferrara[b], I-44100 Ferrara, Italy
[27]INFN Laboratori Nazionali di Frascati, I-00044 Frascati, Italy
[28]INFN Sezione di Genova[a]; Dipartimento di Fisica, Università di Genova[b], I-16146 Genova, Italy
[29]Harvard University, Cambridge, Massachusetts 02138, USA

[30]Universität Heidelberg, Physikalisches Institut, Philosophenweg 12, D-69120 Heidelberg, Germany
[31]Humboldt-Universität zu Berlin, Institut für Physik, Newtonstr. 15, D-12489 Berlin, Germany
[32]Imperial College London, London, SW7 2AZ, United Kingdom
[33]University of Iowa, Iowa City, Iowa 52242, USA
[34]Iowa State University, Ames, Iowa 50011-3160, USA
[35]Johns Hopkins University, Baltimore, Maryland 21218, USA
[36]Laboratoire de l'Accélérateur Linéaire, IN2P3/CNRS et Université Paris-Sud 11, Centre Scientifique d'Orsay, B. P. 34, F-91898 Orsay Cedex, France
[37]Lawrence Livermore National Laboratory, Livermore, California 94550, USA
[38]University of Liverpool, Liverpool L69 7ZE, United Kingdom
[39]Queen Mary, University of London, London, E1 4NS, United Kingdom
[40]University of London, Royal Holloway and Bedford New College, Egham, Surrey TW20 0EX, United Kingdom
[41]University of Louisville, Louisville, Kentucky 40292, USA
[42]Johannes Gutenberg-Universität Mainz, Institut für Kernphysik, D-55099 Mainz, Germany
[43]University of Manchester, Manchester M13 9PL, United Kingdom
[44]University of Maryland, College Park, Maryland 20742, USA
[45]University of Massachusetts, Amherst, Massachusetts 01003, USA
[46]Massachusetts Institute of Technology, Laboratory for Nuclear Science, Cambridge, Massachusetts 02139, USA
[47]McGill University, Montréal, Québec, Canada H3A 2T8
[48]INFN Sezione di Milano[a]; Dipartimento di Fisica, Università di Milano[b], I-20133 Milano, Italy
[49]University of Mississippi, University, Mississippi 38677, USA
[50]Université de Montréal, Physique des Particules, Montréal, Québec, Canada H3C 3J7
[51]Mount Holyoke College, South Hadley, Massachusetts 01075, USA
[52]INFN Sezione di Napoli[a]; Dipartimento di Scienze Fisiche, Università di Napoli Federico II[b], I-80126 Napoli, Italy
[53]NIKHEF, National Institute for Nuclear Physics and High Energy Physics, NL-1009 DB Amsterdam, The Netherlands
[54]University of Notre Dame, Notre Dame, Indiana 46556, USA
[55]Ohio State University, Columbus, Ohio 43210, USA
[56]University of Oregon, Eugene, Oregon 97403, USA
[57]INFN Sezione di Padova[a]; Dipartimento di Fisica, Università di Padova[b], I-35131 Padova, Italy
[58]Laboratoire de Physique Nucléaire et de Hautes Energies, IN2P3/CNRS, Université Pierre et Marie Curie-Paris6, Université Denis Diderot-Paris7, F-75252 Paris, France
[59]University of Pennsylvania, Philadelphia, Pennsylvania 19104, USA
[60]INFN Sezione di Perugia[a]; Dipartimento di Fisica, Università di Perugia[b], I-06100 Perugia, Italy
[61]INFN Sezione di Pisa[a]; Dipartimento di Fisica, Università di Pisa[b]; Scuola Normale Superiore di Pisa[c], I-56127 Pisa, Italy
[62]Princeton University, Princeton, New Jersey 08544, USA
[63]INFN Sezione di Roma[a]; Dipartimento di Fisica, Università di Roma La Sapienza[b], I-00185 Roma, Italy
[64]Universität Rostock, D-18051 Rostock, Germany
[65]Rutherford Appleton Laboratory, Chilton, Didcot, Oxon, OX11 0QX, United Kingdom
[66]CEA, Irfu, SPP, Centre de Saclay, F-91191 Gif-sur-Yvette, France
[67]University of South Carolina, Columbia, South Carolina 29208, USA
[68]Stanford Linear Accelerator Center, Stanford, California 94309, USA
[69]Stanford University, Stanford, California 94305-4060, USA
[70]State University of New York, Albany, New York 12222, USA
[71]University of Tennessee, Knoxville, Tennessee 37996, USA
[72]University of Texas at Austin, Austin, Texas 78712, USA
[73]University of Texas at Dallas, Richardson, Texas 75083, USA
[74]INFN Sezione di Torino[a]; Dipartimento di Fisica Sperimentale, Università di Torino[b], I-10125 Torino, Italy
[75]INFN Sezione di Trieste[a]; Dipartimento di Fisica, Università di Trieste[b], I-34127 Trieste, Italy
[76]IFIC, Universitat de Valencia-CSIC, E-46071 Valencia, Spain
[77]University of Victoria, Victoria, British Columbia, Canada V8W 3P6
[78]Department of Physics, University of Warwick, Coventry CV4 7AL, United Kingdom
[79]University of Wisconsin, Madison, Wisconsin 53706, USA

(Dated: July 10, 2008)

An analysis of exclusive charmless semileptonic B-meson decays based on 383 million $B\overline{B}$ pairs recorded at the $\Upsilon(4S)$ resonance with the *BABAR* detector is presented. Reconstructing the ω mesons in the channel $\omega \to \pi^+\pi^-\pi^0$ and the η mesons in the channels $\eta \to \pi^+\pi^-\pi^0$ and $\eta \to \gamma\gamma$, the branching fractions $\mathcal{B}(B^+ \to \omega\ell^+\nu) = (1.18 \pm 0.17_{stat} \pm 0.08_{syst}) \times 10^{-4}$ and $\mathcal{B}(B^+ \to \eta\ell^+\nu) = (3.19 \pm 0.61_{stat} \pm 0.80_{syst}) \times 10^{-5}$ are measured.

PACS numbers: 13.20.He, 14.40.Nd

Measurements of branching fractions of charmless semileptonic B decays can be used to determine the Cabibbo-Kobayashi-Maskawa matrix [1] element $|V_{ub}|$ and thus provide an important constraint on the Unitarity Triangle. Studies of exclusive decays allow for more stringent kinematical constraints and better background suppression than inclusive measurements. The determination of $|V_{ub}|$ from branching-fraction measurements of exclusive decays depends on theoretical predictions of form factors and is thus affected by theoretical uncertainties that are different from those involved in inclusive decays. The currently most precise determination of $|V_{ub}|$ using exclusive decays comes from a *BABAR* measurement of $B \to \pi \ell \nu$ decays [2]. It is important to study other semileptonic final states to perform further tests of theoretical calculations and to improve the knowledge of the composition of charmless semileptonic decays.

In this paper, new measurements of the branching fractions $\mathcal{B}(B^+ \to \omega \ell^+ \nu)$ and $\mathcal{B}(B^+ \to \eta \ell^+ \nu)$ (charge-conjugate modes are included implicitly) are presented. These decays have previously been studied by the CLEO [3] and *BABAR* [4, 5] collaborations ($B^+ \to \eta \ell^+ \nu$) and by the Belle [6] collaboration ($B^+ \to \omega \ell^+ \nu$). The ω meson is reconstructed in its decay to three pions ($\mathcal{B}(\omega \to \pi^+\pi^-\pi^0) = (89.1 \pm 0.7)\%$ [7]), while for the η meson the decay to three pions and the decay to two photons ($\mathcal{B}(\eta \to \pi^+\pi^-\pi^0) = (22.7 \pm 0.4)\%$, $\mathcal{B}(\eta \to \gamma\gamma) = (39.38 \pm 0.24)\%$ [7]) are used. In contrast to earlier $B^+ \to \eta \ell^+ \nu$ analyses in *BABAR* [4, 5], this measurement does not reconstruct the second B meson in the event and therefore yields a much larger candidate sample.

The results presented here are based on a sample of 383 million $B\overline{B}$ pairs recorded with the *BABAR* detector [8] at the PEP-II asymmetric-energy e^+e^- storage rings. The data correspond to an integrated luminosity of 347 fb^{-1} collected at the $\Upsilon(4S)$ resonance and 35 fb^{-1} recorded 40 MeV below the resonance (off-resonance). Simulated $B\overline{B}$ events are used to estimate signal efficiencies and shapes of signal and background distributions. Charmless semileptonic decays are simulated as a mixture of three-body decays $B \to X_u \ell \nu$ ($X_u = \pi, \eta, \eta', \rho, \omega$) and have been reweighted according to the latest form-factor calculations from light-cone sum rules [9–11]. Decays to non-resonant hadronic states X_u with masses $m_{X_u} > 2m_\pi$ are simulated following a prescription of Ref. [12]. Monte-Carlo simulations based on `GEANT` 4 [13] are used to model the *BABAR* detector response, taking into account the varying detector conditions.

The reconstruction of the signal decays $B^+ \to \omega \ell^+ \nu$ and $B^+ \to \eta \ell^+ \nu$ requires the identification of a charged lepton ($\ell = e, \mu$) and the reconstruction of an ω or η meson. The center-of-mass momentum of the lepton is restricted to $|\vec{p}^{\,*}_\ell| > 1.6$ (1.0) GeV [14] for the ω (η) final state. This lepton-momentum requirement significantly reduces the background with fake leptons and rejects a large fraction of true leptons from secondary decays or photon conversions. For the reconstruction of the ω or η meson, charged (neutral) pions are required to have a momentum in the laboratory frame above 200 (400) MeV to reduce combinatorial background. Neutral pion candidates are formed from two photons with energies above 100 MeV and an invariant mass in the range $100 < m_{\gamma\gamma} < 160\,\text{MeV}$. A three-pion system is accepted as an ω (η) candidate if its invariant mass is in the range $760 < m_{3\pi} < 806\,\text{MeV}$ for ω candidates and $540 < m_{3\pi} < 555\,\text{MeV}$ for η candidates. The η meson is also reconstructed via its decay into two photons, for which photon energies above 50 MeV and a two-photon invariant mass in the range $520 < m_{\gamma\gamma} < 570\,\text{MeV}$ are required. To reduce the combinatorial background, two-photon combinations are rejected as possible η candidates if one of the photons can be combined with any other photon of the event to form a π^0.

The charged lepton is combined with an $\omega(\eta)$ candidate to form a so-called Y pseudo-particle candidate, whose four-momentum is defined as the sum of the corresponding lepton and hadron four-momenta. All charged tracks belonging to the Y are fit to a common vertex. This vertex fit must yield a χ^2 probability of at least 0.1%. Multiple Y candidates per event are possible and all candidates are retained in this analysis. The Y multiplicity is well described by the Monte-Carlo simulation; about 96% (98%) of simulated $B^+ \to \omega \ell^+ \nu$ ($B^+ \to \eta \ell^+ \nu$) signal events and more than 90% of all selected data events contain only one Y candidate.

The neutrino four-momentum, $P_\nu = (|\vec{p}_{\text{miss}}|, \vec{p}_{\text{miss}})$, is inferred from the difference between the net momentum of the colliding-beam particles and the sum of the momenta of all detected particles in the event. Here the modulus of the missing-momentum vector is used to estimate the neutrino energy, since the missing momentum is a vector sum and contributions from particle losses or additional tracks or energy deposits do not add linearly as is the case for the missing energy. Hence the missing momentum tends to have a better resolution than the measured missing energy. A minimum value for the modulus of the missing-momentum vector of 500 MeV is required. To reduce the effect of losses due to detector acceptance, the missing-momentum vector must point into the polar-angle range $0.3 < \theta_{\text{miss}} < 2.2$ rad. If the missing energy and momentum in the event comes from a single undetected neutrino and the rest of the event is correctly reconstructed, the missing mass measured from the whole event should be compatible with zero. Because the missing-mass resolution varies linearly with the missing energy, only events with $|m^2_{\rm miss}/(2E_{\rm miss})| < 2.5$ GeV are selected.

Assuming a vanishing missing mass, the angle between the Y candidate and the B meson is computed as $\cos\theta_{BY} = \left(2E^*_B E^*_Y - M^2_B - M^2_Y\right) / \left(2|\vec{p}^*_B||\vec{p}^*_Y|\right)$. Here $M_B, M_Y, E^*_B, E^*_Y, \vec{p}^*_B, \vec{p}^*_Y$ refer to the masses, energies, and momenta of the B meson and the Y candidate. The B-meson energy E^*_B and momentum $\vec{p}^*_B$ are not measured event by event. Instead, $E^*_B = \sqrt{s}/2$ is given by the center-of-mass energy of the colliding beam particles, and the modulus of the B momentum is derived as $|\vec{p}^*_B| = \sqrt{E^{*2}_B - m^2_B}$. Signal candidates are required to satisfy $-1.2 < \cos\theta_{\rm BY} < 1.1$, allowing for detector resolution and photon radiation.

To enhance signal over background, the momenta of the lepton ($\vec{p}^*_\ell$) and the hadron ($\vec{p}^*_{\omega,\eta}$) that make up a Y candidate are restricted. For $B^+ \to \omega\ell^+\nu$, the momenta are required to satisfy $|\vec{p}^*_\omega| > 1.3$ GeV or $|\vec{p}^*_\ell| > 2.0$ GeV or $|\vec{p}^*_\omega| + |\vec{p}^*_\ell| > 2.65$ GeV. In the case of $B^+ \to \eta\ell^+\nu$, the conditions $|\vec{p}^*_\eta| > 1.3$ GeV or $|\vec{p}^*_\ell| > 2.1$ GeV or $|\vec{p}^*_\eta| + |\vec{p}^*_\ell| > 2.8$ GeV have to be fulfilled.

Event-shape variables that are sensitive to the topological differences between jet-like continuum events and more spherical $B\bar{B}$ events are used to suppress backgrounds from $e^+e^- \to q\overline{q}\,(q = u, d, s, c)$ and other QED processes. The second Fox-Wolfram moment R_2 [15] is required to be less than 0.5 and a loose requirement on the second Legendre moment L_2 [16] of $L_2 < 3.0$ GeV is imposed. In addition, the event must contain at least four charged tracks.

The kinematic consistency of the $Y + \nu$ system with a signal B decay is checked using the two variables $\Delta E = (P_B \cdot P_{\rm beam} - s/2)/\sqrt{s}$ and $m_{\rm ES} = \sqrt{(s/2 + \vec{p}_B \cdot \vec{p}_{\rm beam})^2/E^2_{\rm beam} - \vec{p}^2_B}$, where $\sqrt{s}$ is the center-of-mass energy of the colliding beam particles and $P_B = (E_B, \vec{p}_B)$ is the B-meson four-momentum. Only candidates with $|\Delta E| < 0.95$ GeV and $m_{\rm ES} > 5.095$ GeV are retained. In addition, these variables are later used to extract the signal yields in a fit to the two-dimensional ΔE vs. $m_{\rm ES}$ distribution.

At this stage of the selection, the signal-to-background ratio is low and amounts to 0.8% for $B^+ \to \omega\ell^+\nu$, and 0.2% (1.0%) for $B^+ \to \eta\ell^+\nu$ with $\eta \to \pi^+\pi^-\pi^0(\gamma\gamma)$. The total signal efficiencies for the sum of electrons and muons are 4.1% for $B^+ \to \omega\ell^+\nu$ and 8.5% (16%) for $B^+ \to \eta\ell^+\nu$ where the η decays in three pions (two photons).

To further discriminate the signal against the background, a multivariate selection based on neural networks [17] is used. For each of the three signal channels under study, neural-networks with two hidden layers (four and two neurons, respectively) are applied consecutively to separate the signal from the two main backgrounds. A first neural network discriminates the signal against $q\overline{q}$ continuum events; a second network is used to further distinguish the signal from the $B \to X_c\ell\nu$ background. The neural-network decision is based on the following input variables: $m^2_{miss}/(2E_{miss})$, θ_{miss}, $\cos\theta_{BY}$, R_2, L_2, $\cos\Delta\theta_{thrust}$, the cosine of the polar-angle difference between the thrust axis of the Y candidate and the thrust axis of the rest of the event, and $\cos\theta_{W\ell}$, the cosine of the lepton "helicity angle" measured in the rest frame of the virtual W relative to the W direction in the laboratory frame. For the three-pion final states, the Dalitz amplitude, the outer product of the π^+ momentum vector and the π^- momentum vector in the ω/η rest frame, normalized to its maximum value, serves as an additional input variable.

TABLE I: Efficiencies and signal-to-background ratios after the neural-network selection. The signal-to-background ratio is shown both in the ΔE vs. m_{ES} range used in the selection ("fit region") and for illustration purposes also in a smaller region with enhanced signal fraction, delimited by $-0.2 < \Delta E < 0.4$ GeV and $m_{ES} > 5.255$ GeV ("signal region").

	Fit Region		Signal Region
	ϵ_{signal}	S/B	S/B
$B^+ \to \omega\ell^+\nu$	0.12	0.136	0.43
$B^+ \to \eta\ell^+\nu$, $\eta \to \pi^+\pi^-\pi^0$	0.56	0.097	0.34
$B^+ \to \eta\ell^+\nu$, $\eta \to \gamma\gamma$	2.56	0.036	0.14

The training of the neural networks is done using the corresponding simulated signal and background samples for each of the three signal channels separately. Independent simulated event samples are used to validate the training. Based on Monte-Carlo simulation, a selection criterion for each of the output discriminants is chosen to maximize the expected statistical significance, $S/\sqrt{S+B}$, where S and B denote the expected signal and background yields, respectively. The signal efficiencies and the estimated S/B ratios after the neural-network selection are given in Table I.

To extract the signal yields, binned extended maximum-likelihood fits [18] to the ΔE vs. $m_{\rm ES}$ distributions of the three signal channels in the range defined above are performed independently. The fit accounts for statistical fluctuations of the data and Monte-Carlo samples and determines the relative proportions of signal and background samples describing the data. The fit uses a total of 50 bins with small bin sizes in the region around the signal peak to resolve the signal shape and larger bin sizes in the sidebands to determine the background normalization from data.

Free parameters of the fit are the normalizations of the signal and the $B \to X_c\ell\nu$ background samples. The $B \to X_c\ell\nu$ background normalization is left free to account for a slight discrepancy of the $B \to X_c\ell\nu$ background yields between data and Monte-Carlo simulation. For $B^+ \to \omega\ell^+\nu$, it was found that the $q\bar{q}$ continuum background can also be estimated from the fit to the data. Its normalization is thus left free in the fit. For the $B^+ \to \eta\ell^+\nu$ channels, where the signal-to-background ratio is worse and the correlations between the back-

TABLE II: Total branching fractions obtained from the maximum-likelihood fits for the three signal channels and the combined $B^+ \to \eta\ell^+\nu$ channels. The last row shows the χ^2 per degree of freedom to estimate the quality of the fit results.

	$B^+ \to \omega\ell^+\nu$	$B^+ \to \eta\ell^+\nu$		
		$\eta \to \pi^+\pi^-\pi^0$	$\eta \to \gamma\gamma$	combined
$\mathcal{B}(10^{-5})$	11.8 ± 1.7	4.53 ± 1.48	3.08 ± 0.67	3.19 ± 0.61
$\chi^2/d.o.f.$	50.2/47	53.8/48	26.9/48	26.3/48

grounds are rather high, the amount of $q\bar{q}$ background is determined from off-resonance data and is not varied in the fit. All other background distributions are fixed to their Monte-Carlo predictions. Table II presents the fit results in terms of signal branching fractions for the three signal channels. As for the background, the fit adjusts the $B \to X_c\ell\nu$ normalization with respect to the Monte-Carlo simulation by a factor of 1.06 ± 0.07 for $B^+ \to \omega\ell^+\nu$ and 0.96 ± 0.07 (1.12 ± 0.03) for $B^+ \to \eta\ell^+\nu$ with $\eta \to \pi^+\pi^-\pi^0$ ($\eta \to \gamma\gamma$). The correlations between the signal and the $B \to X_c\ell\nu$ fit parameters are 0.08, -0.60, and -0.48 for the above signal channels, respectively. The correlation between the signal and the continuum fit parameters for the $B^+ \to \omega\ell^+\nu$ channel is -0.55 and the continuum background is adjusted by a factor of 0.89 ± 0.12 with respect to the normalization obtained from the low-statistics off-resonance data sample. The goodness-of-fit is evaluated using a χ^2-based comparison of the fitted simulated ΔE vs. $m_{\rm ES}$ distributions and data and is shown in Table II. In addition, the ΔE vs. $m_{\rm ES}$ distributions of the two η channels have been added and fitted together to obtain a combined branching fraction measurement for $B^+ \to \eta\ell^+\nu$. The results of the combined fit are also presented in Table II.

Figure 1 shows projections of the fitted ΔE vs. m_{ES} distributions for the three signal channels and the combined $B^+ \to \eta\ell^+\nu$ channel. For illustration purposes, the signal contribution is enhanced by restricting the events to $-0.2 < \Delta E < 0.4\,\mathrm{GeV}$ for the m_{ES} distributions and to $m_{ES} > 5.255\,\mathrm{GeV}$ for the ΔE distributions.

All the systematic errors on the measured branching fractions are listed in Table III. To estimate them, each variable in the description of the detector efficiencies and in the modeling of the signal and the background processes is varied within its uncertainty. The complete analysis is then repeated and the differences in the resulting branching fractions are taken as the systematic error for this specific variable. The total systematic error is then computed as the quadratic sum of all the listed contributions.

Uncertainties due to the reconstruction of charged particles and photons are evaluated by varying in simulation their reconstruction efficiencies and the energy depositions of photons. The neutrino reconstruction is affected by long-lived K_L^0, which often escape detection and contribute to the measured missing momentum of the event. The uncertainty arising from the assumed K_L^0 production rate and the description of the K_L^0 detection is estimated by varying their production rate as well as their detection efficiency and energy deposition in the simulation. For lepton identification, relative uncertainties of 1.4% and 3% are used for electrons and muons, respectively. A 3% uncertainty is assigned to the $\pi^0/\eta \to \gamma\gamma$ reconstruction efficiency.

The uncertainty due the $B \to X_c\ell\nu$ background is evaluated by varying the $B \to D/D^*/D^{**}\ell\nu$ branching fractions [7] and the $B \to D^*$ form factors [19]. Prior to the event selection by the neural networks, the background level is high and discrepancies between data and Monte-Carlo distributions of the neural-network input variables are observed. To estimate the effect of these discrepancies on the measured branching fractions, the dominant background component, the $B \to X_c\ell\nu$ events, is reweighted. The weights are determined from a $B \to X_c\ell\nu$-enhanced sample obtained by selecting only events that are otherwise rejected by the $B \to X_c\ell\nu$ neural-network selection, but keeping all other selection requirements unchanged.

For the $B \to X_u\ell\nu$ background, the non-resonant contribution is varied within the range allowed by the uncertainty of the total $B \to X_u\ell\nu$ branching fraction [20]. The uncertainty due to the normalization of the continuum background is determined with off-resonance data.

Uncertainties in the modeling of signal decays due to the imperfect knowledge of the form factors affect the shapes of kinematic spectra and thus the acceptances of signal decays. This has an effect on the measured branching fractions. As the ω meson is a vector meson, the $B^+ \to \omega\ell^+\nu$ decay is described by three form factors, for which the parametrization of [10] is used. The $B^+ \to \eta\ell^+\nu$ decay is described by a single form factor [11], since the η meson is a pseudoscalar meson. In both cases, the errors on the measured branching fractions due to form-factor shapes is estimated by varying the parameters of the form-factor calculations withing their uncertainties. The branching fractions of the decays $\omega/\eta \to \pi^+\pi^-\pi^0$ and $\eta \to \gamma\gamma$ are varied within their uncertainties [7]. The uncertainty on the number of produced B mesons has been measured to be 1.1 %.

The total systematic error on the measured branching fractions amounts to 7.1 % and 25.1 % for the $B^+ \to \omega\ell^+\nu$ and the combined $B^+ \to \eta\ell^+\nu$ channels, respectively.

In summary, the exclusive total branching fractions of $B^+ \to \omega\ell^+\nu$ and $B^+ \to \eta\ell^+\nu$ decays have been measured to be

$$\mathcal{B}(B^+ \to \omega\ell^+\nu) = (1.18 \pm 0.17 \pm 0.08) \times 10^{-4},$$
$$\mathcal{B}(B^+ \to \eta\ell^+\nu) = (3.19 \pm 0.61 \pm 0.80) \times 10^{-5},$$

where the errors are statistical (data and simulation) and systematic.

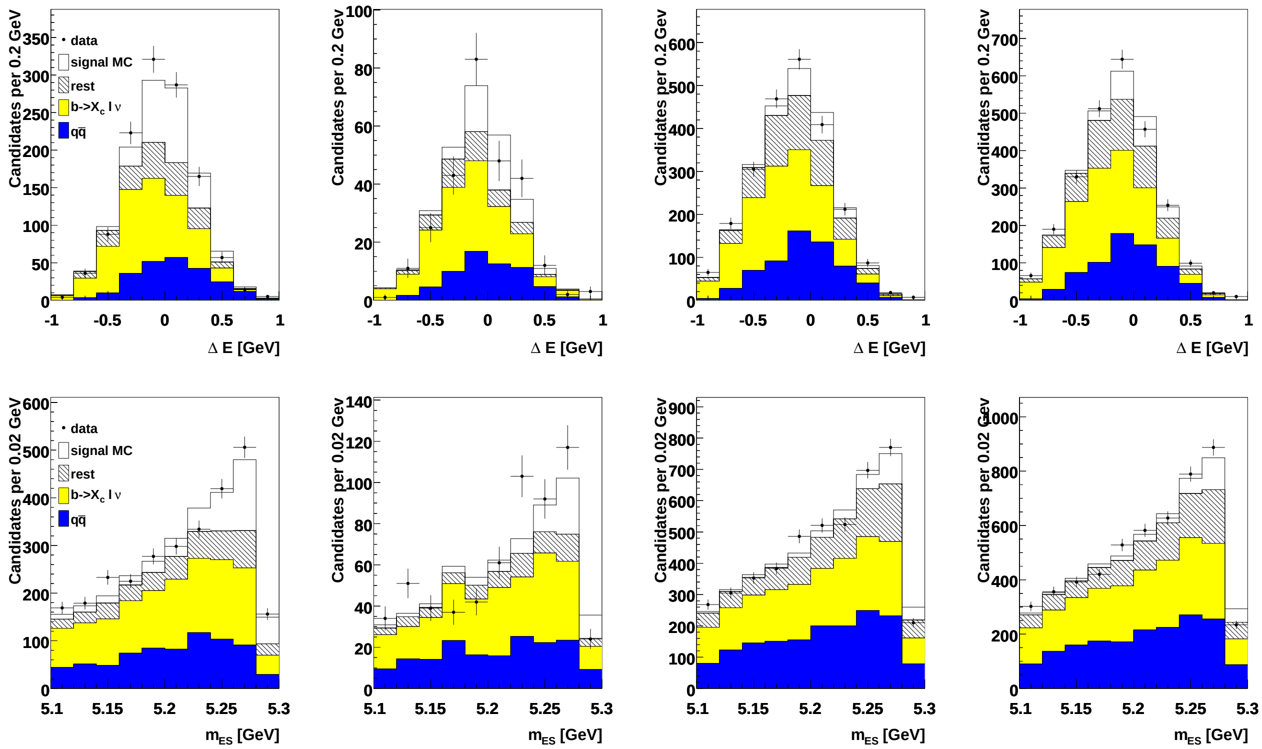

FIG. 1: (color online) Projected ΔE distributions for $m_{\rm ES} > 5.255$ GeV (top), and m_{ES} distributions for $-0.2 < \Delta E < 0.4$ GeV (bottom). From left to right: $B^+ \to \omega\ell^+\nu$ channel, $B^+ \to \eta\ell^+\nu$ channel with $\eta \to \pi^+\pi^-\pi^0$, $B^+ \to \eta\ell^+\nu$ channel with $\eta \to \gamma\gamma$, and combined $B^+ \to \eta\ell^+\nu$ channels. The error bars on the data points represent the statistical uncertainties. The histograms show simulated distributions for signal (white), $B \to X_c\ell\nu$ decays (light shaded/yellow), $q\bar{q}$-continuum (dark shaded/blue) and all other backgrounds (hatched). The distributions of the simulated signal and $B \to X_c\ell\nu$ background have been scaled to the results of the maximum-likelihood fit.

The $B^+ \to \omega\ell^+\nu$ result significantly improves the current knowledge of this decay. For comparison, the previously most precise measurement by the Belle [6] collaboration yielded $\mathcal{B}(B^+ \to \omega\ell^+\nu) = 1.3 \pm 0.4_{stat} \pm 0.4_{syst}$. The $B^+ \to \eta\ell^+\nu$ result is compatible with and comparable in relative precision to the currently best measurement by *BABAR* [5] based on semileptonic B-tags, $\mathcal{B}(B^+ \to \eta\ell^+\nu) = 6.4 \pm 2.0_{stat} \pm 0.3_{syst} \times 10^{-5}$. The analysis presented here is statistically independent and thus complements the semileptonic-tag measurement. It is statistically more precise but has larger systematic uncertainties, as expected for an untagged measurement. The improved measurements of $B^+ \to \omega\ell^+\nu$ and $B^+ \to \eta\ell^+\nu$ decays are important ingredients in the understanding of the composition of the inclusive charmless semileptonic decay rate.

We are grateful for the excellent luminosity and machine conditions provided by our PEP-II colleagues, and for the substantial dedicated effort from the computing organizations that support *BABAR*. The collaborating institutions wish to thank SLAC for its support and kind hospitality. This work is supported by DOE and NSF (USA), NSERC (Canada), IHEP (China), CEA and CNRS-IN2P3 (France), BMBF and DFG (Germany), INFN (Italy), FOM (The Netherlands), NFR (Norway), MIST (Russia), and PPARC (United Kingdom). Individuals have received support from CONACyT (Mexico), A. P. Sloan Foundation, Research Corporation, and Alexander von Humboldt Foundation.

---

* Deceased
† Now at Temple University, Philadelphia, Pennsylvania 19122, USA
‡ Now at Tel Aviv University, Tel Aviv, 69978, Israel
§ Also with Università di Perugia, Dipartimento di Fisica, Perugia, Italy
¶ Also with Università di Roma La Sapienza, I-00185 Roma, Italy
** Now at University of South Alabama, Mobile, Alabama 36688, USA
†† Also with Università di Sassari, Sassari, Italy

[1] M. Kobayahi, T. Maskawa, Prog. Theor. Phys. **49**, 652 (1973).
[2] B. Aubert *et al.*, Phys. Rev. Lett. **98**, 091801 (2007).
[3] CLEO Collaboration, S.B. Athar *et al.*, Phys. Rev. **D68**,

TABLE III: Relative systematic errors of the branching fractions $\mathcal{B}(B^+ \to \omega\ell^+\nu)$ and $\mathcal{B}(B^+ \to \eta\ell^+\nu)$. For the $B^+ \to \eta\ell^+\nu$ channel, the systematics errors for the three-pion and the two-photon final states as well as for the combined result is shown. The total error in each column is the sum in quadrature of all listed contributions.

	$\delta\mathcal{B}(B^+ \to \omega\ell^+\nu)$ (%)	$\delta\mathcal{B}(B^+ \to \eta\ell^+\nu)$ (%)		
		$(\eta \to \pi^+\pi^-\pi^0)$	$(\eta \to \gamma\gamma)$	combined
Tracking efficiency	1.9	4.9	4.2	4.6
Photon reconstruction	2.1	1.8	9.1	8.6
K_L^0 Production and Interactions	2.6	4.8	3.1	1.9
Lepton Identification	1.9	3.3	6.9	6.3
π^0/η Identification	3.8	6.9	13.3	12.2
Neural-Net Input Variables	0.6	0.8	5.9	6.1
D^* Form Factor	0.4	1.0	0.9	1.0
$\mathcal{B}(B \to X_c\ell\nu)$	2.1	5.5	7.6	8.0
$\mathcal{B}(B \to X_u\ell\nu)$	2.8	4.4	9.8	8.6
Continuum Scaling	0.7	15.8	10.4	12.7
Signal Form Factor	1.8	5.9	0.3	1.3
$\mathcal{B}(\omega/\eta \to X)$	0.8	1.5	0.6	1.2
$N_{B\bar{B}}$	1.1	1.1	1.1	1.1
Total Systematic Error	7.1	21.1	25.2	25.1

072003 (2003); CLEO Collaboration, D. M. Asner *et al.*, Phys. Rev. **D76**, 012007 (2007).

[4] *BABAR* Collaboration, B. Aubert *et al.*, hep-ex/0607066 (contribution to ICHEP, Moscow, 2006).

[5] *BABAR* Collaboration, B. Aubert *et al.*, SLAC-PUB-1321, arXiv:0805.2408 [hep-ex] (submitted to Phys. Rev. Lett.).

[6] Belle Collaboration, C. Schwanda *et al.*, Phys. Rev. Lett. **93**, 131803 (2004).

[7] W.-M. Yao et al., The Review of Particle Physics, Journal of Physics G 33, 1 (2006).

[8] *BABAR* Collaboration, B. Aubert *et al.*, Nucl. Instrum. Methods Phys. Research **A479**, 1 (2002).

[9] P. Ball, R. Zwicky, Phys. Rev. **D71**, 014015 (2005).

[10] P. Ball, R. Zwicky, Phys. Rev. **D71**, 014029 (2005).

[11] P. Ball, G.W. Jones, arXiv:hep-ph/0412079v1 (2007).

[12] F. De Fazio, M. Neubert, JHEP **9906**, 017 (1999).

[13] GEANT Collaboration, S. Agostinelli *et al.*, Nucl. Instrum. Methods Phys. Sec. **A506**, 250 (2003).

[14] All variables denoted with a star (e.g. p^*) are given in the $\Upsilon(4S)$ rest frame; all others are given in the laboratory frame.

[15] $R_2 = \sum_{ij} |p_i||p_j|P_2(cos\Theta_{ij})$, where the summation is over all final state particles, p_i and p_j are momenta of the particles i and j, Θ_{ij} is the angle between them and $P_2(x) = (1/2)(3x^2 - 1)$ is the second Legendre polynomial.

[16] $L_2 = \sum_i |\vec{p}_i^*| \cos^2(\Theta_i^*)$, where the sum is over all tracks in the event not used to form the Y candidate and $\vec{p}_i^*$ and Θ_i^* are their momenta and angles with respect to the thrust axis of the Y candidate, respectively.

[17] A. Höcker *et al.*, arXiv:physics/0703039v4 [physics.data-an].

[18] R. J. Barlow, C. Beeston, Comput. Phys. Commun. **77**, 219 (1993).

[19] *BABAR* Collaboration, B. Aubert *et al.*, Phys. Rev. **D77**, 032002 (2008).

[20] Heavy Flavor Averaging Group, http://www.slac.stanford.edu/xorg/hfag/.